Development 127, 893-905 (2000)
Printed in Great Britain © The Company of Biologists Limited 2000
DEV2501

The growth of the dermomyotome and formation of early myotome lineages in thoracolumbar somites of chicken embryos

Wilfred F. Denetclaw, Jr and Charles P. Ordahl*

Department of Anatomy and Cardiovascular Research Institute, University of California San Francisco, San Francisco, CA 94143, USA

*Author for correspondence (e-mail: ordahl@itsa.ucsf.edu)

Accepted 16 November 1999; published on WWW 26 January 2000

SUMMARY

Myotome formation in the epaxial and hypaxial domains of thoraco-lumbar somites was analyzed using fluorescent vital dye labeling of dermomyotome cells and cell-fate assessment by confocal microscopy. Muscle precursor cells for the epaxial and hypaxial myotomes are predominantly located in the dorsomedial and ventrolateral dermomyotome lips, respectively, and expansion of the dermomyotome is greatest along its mediolateral axis coincident with the dorsalward and ventralward growth directions of the epaxial and hypaxial myotomes. Measurements of the dermomyotome at different stages of development shows that myotome growth begins earlier in the epaxial than in the hypaxial domain, but that after an initial lag phase, both progress at the same rate. A combination of dye injection and/or antibody labeling of early and late-expressed muscle contractile proteins confirms the myotome mediolateral growth directions, and shows that the myotome thickness increases in a superficial (near dermis) to deep (near sclerotome) growth direction. These findings also provide a basis for predicting the following gene expression sequence program for the earliest muscle precursor lineages in mouse embryos: *Pax-3* (stem cells), *myf-5* (myoblast cells) and *myoD* (myocytes). The movements and mitotic activity of early muscle precursor cells lead to the conclusion that patterning and growth in the myotome specifically, and in the epaxial and hypaxial domains of the body generally, are governed by morphogenetic cell movements.

Key words: Dye fate mapping, Confocal microscopy, Skeletal muscle, French Flag Model, Morphogenesis, Embryonic fields, Morphogenetic cell movements

INTRODUCTION

Somites, paired epithelial spheres on either side of the axial neural tube and notochord, form by condensation of the segmental plate mesoderm at its cranial end, producing, in the case of chick, 50 somite pairs at a rate of one somite every 90 minutes (Palmeirim et al., 1997). The sequential formation of somites in a caudo-cranial direction imparts a progressive cranial directed maturation gradient which can be defined in terms of somite stages to mark somite axial position with specific developmental events during early embryo development (Ordahl, 1993). The newly formed, stage 1 somite (ss1) is epithelial and is patterned along its initial dorsoventral, cranio-caudal, and mediolateral axes in response to local signals from surrounding tissues (Christ and Ordahl, 1995; Christ et al., 1992). The first molecular evidence of dorsoventral patterning is the suppression of *Pax-3* gene expression in the ventral half of the epithelium of the newly formed somite (Williams and Ordahl, 1994; Goulding et al., 1994; Bober et al., 1994). The first cellular evidence of dorsoventral patterning occurs as the ventral half of the somite undergoes an epithelial-mesenchymal transition to form the sclerotome. Ventral axial signals from the notochord and floor plate of the neural tube have been implicated in this patterning, inducing both the cellular transformation (Brand-Saberi et al., 1993; Koseki et al., 1993; Pourquie et al., 1993) and associated changes in gene expression (Fan and Tessier-Lavigne, 1994; Dietrich et al., 1997). A major signal moiety from these axial structures is the enigmatic Sonic Hedgehog gene product that is sufficient in vitro to elicit activation of the *Pax-1* gene in somite explant culture (Fan and Tessier-Lavigne, 1994) but remains controversial as to whether it acts as an inducer, in the classical embryological sense, or as a growth/survival factor necessary for the expression of endogenous cell fate programs (Teillet and Le Douarin, 1983; Teillet et al., 1998).

Dorsally, the neural tube and the surface ectoderm signals also act locally, through secretion of Wnt proteins and intercellular contacts, to maintain the dorsal somite epithelium, the dermomyotome, and to maintain its potential for myogenesis (Meunsterberg et al., 1995; Stern et al., 1995; Spence et al., 1996; Fan et al., 1997; Marcelle et al., 1997; Dietrich et al., 1997). In histological section, the simple pseudostratified columnar epithelium of the dermomyotome recurves at the interfaces with the ventral sclerotome forming boundaries or lips, where dermomyotome cells lose their columnar morphology but remain contained within the basal lamina (Tosney et al., 1994). As tissues grow and expand, the medial lip of the dermomyotome maintains its close

association with the dorsal neural tube and the ectoderm, and coming to lie more dorsally is variously referred to as the dorsal lip or medial lip. To avoid confusion we will refer to this lip as the dorsomedial lip and similarly to the opposite dermomyotome boundary as the ventrolateral lip. In somites at limb levels, the cells along the ventrolateral lip escape the confines of the basal lamina and migrate to the adjacent limb bud (Fischel, 1895; Christ et al., 1974, 1977; Jacob et al., 1978, 1979) where they will become skeletal myocytes (Christ et al., 1977; Kieny et al., 1988). At the dorsomedial lip, by contrast, dermomyotome cells translocate to the subjacent myotome layer and begin to differentiate as primary myocytes within the epaxial myotome (Williams, 1910; Kaehn et al., 1988; Denetclaw et al., 1997). The dermomyotome also gives rise to the dermatome which forms the dorsal dermis (Brill et al., 1995). Consequently, as the somite is patterned, the dermomyotome is a 2-dimensional epithelial sheet from which emerges the 3-dimensional tissue structure of the body musculature.

In the present paper we have used fluorescent vital dye tracing to follow the lineage and morphogenetic movements of muscle precursor cells in thoraco-lumbar somites. Thoraco-lumbar somites form an epaxial myotome, but unlike their limb-level counterparts, also form a hypaxial myotome which is the primordium of the intercostal and abdominal wall muscles. At the extreme ventrolateral lips of the thoraco-lumbar-level dermomyotome, mononucleated muscle fibers appear that span between the cranial and caudal lips of the somite in a manner similar to that seen for the epaxial myotome. Our analysis shows that the epaxial myotome of thoraco-lumbar somites forms in a manner identical to that of the previously studied wing-level somites. Formation of the hypaxial myotome, rather than occurring through cell migration as in wing-level somites, involves similar cellular translocations as in the epaxial myotome, but precursor cells are deposited from the dermomyotome in an inverted mediolateral pattern. Finally, these results yield new quantitative information regarding growth dynamics and morphogenesis in the dermomyotome field during early embryogenesis.

MATERIALS AND METHODS

Chicken embryo growth and staging

Fertile white leghorn chicken eggs (*Gallus gallus domesticus*), were obtained from a local supplier (Petaluma Farms, Petaluma, CA), and were immediately used or stored for up to 1 week at 4°C. Eggs were incubated on their sides for 2 days at 38.9°C in a humidified incubator. Embryos were then staged (Hamburger and Hamilton, 1951) and somite developmental age was assessed according to Ordahl (1993), except that in this paper Arabic numbers replace Roman numerals (e.g. ss5 = somite stage five [V]).

Confocal microscopy

Somite dermomyotome dye-labeling and antibody detection of muscle proteins has been described previously (Denetclaw et al., 1997). For confocal microscopy, a Nikon PCM2000 confocal scan head was mounted on an Eclipse PhysioStation™ fluorescence microscope (E600FN, Nikon) and used with low magnification dry 10×/0.5 NA and 20×/0.75 NA Fluar objectives or with a high magnification water 40×/0.8 NA Plan-Apo objective. A green helium-neon and argon ion laser combination excited DiI- and DiO-labeled cells, and dye fluorescence was directed to separate photomultiplier tube channels using filter sets for rhodamine and fluorescein fluorochromes, respectively. The C-Imaging™ (Compix, Inc.) operating system packaged with the confocal set up captured time-averaged (Kalman averages) 8-bit images. For all confocal figures, a single composite image was generated from z-axis serial scans (typically 15 images) through the whole dermomyotome and myotome dye-labeled areas. Adobe Photoshop™ 3.0 was used to merge grayscale images for false-color production, and NIH-Image, version 1.61, was used for image processing. Antibodies to muscle structural proteins were polyclonal desmin antibody (BioGenex), monoclonal chicken cardiac C-protein antibody (gift from Dr Takashhi Obinata) and monoclonal myosin heavy chain (HV-11) antibody (gift from Dr Everett Bandman).

Calculation of somite dermomyotome growth rates

Tables 1 and 2 show thoraco-lumbar somite measurements at different stages of chicken embryo growth: HH15-17 (0 hours, fixed immediately after dye-labeling); HH18-19 (fixed 10-20 hours after dye labeling); HH20-23 (fixed 21-30 hours after dye labeling); HH25-26 (fixed 41-50 hours after dye labeling). Whole dermomyotome and epaxial and hypaxial domain somite measurements were made using the C-Imaging™ measurements program on the PCM2000 confocal imaging system.

Dye injections in the dermomyotome dorsomedial and ventrolateral lips resulted in epaxial and hypaxial domain cell labeling after 1 to 2 days of embryo growth, respectively. Measurements of the distribution of dye-labeled dermomyotome and myotome cells in these two domains, as well as the region of unlabeled cells in the dermomyotome intervening space, are presented as mean and standard deviations for different embryo growth periods (Tables 1 and 2). In addition, the autofluorescence of the dermomyotome and the appearance of dark lines outlining its borders allowed the overall growth of the dermomyotome to be determined for its cranio-caudal and mediolateral axes. In all cases, measurements were made at mid-position in the dermomyotome.

In addition to somite size measurements, growth rates (μm/hr) were determined for the dermomyotome and for the specific epaxial, intervening space and hypaxial domains (see Table 2). The changing dimensions of dermomyotome along its mediolateral axis shows that it is expanding exponentially. Therefore, to determine which regions of the dermomyotome account for this rapid increase, individual growth rates were determined for each domain size measurement between 0 and 21-30 hours, and between 21-30 hours and 41-50 hours. The average size of somite domains at HH15-17 and at HH20-23 was subtracted from the individually measured domain sizes at HH20-23 and HH25-26, respectively. Also, the somite growth interval was determined by subtracting 0 or 25 hours (the middle time value between 21-30 hours) from the overall growth times of individual embryos occurring at HH20-23 or HH25-26, respectively. Statistical significance was determined using an unpaired, one-tailed, Student's *t*-test and significance was considered to be $P \leq 0.05$.

RESULTS

The process of epaxial and hypaxial myotome formation is similar, but myotome growth expands in opposite directions

A cellular fate map of early epaxial myotome formation in wingbud level somites previously established the location of myotome precursor cells, the schedule of birthdates of myotome fibers, and the direction of growth of myotome fibers after micro-injection of DiI and DiO along nine specific sites in the dermomyotome and after monitoring for dye-labeled myotome fiber growth by confocal microscopy (Denetclaw et al., 1997).

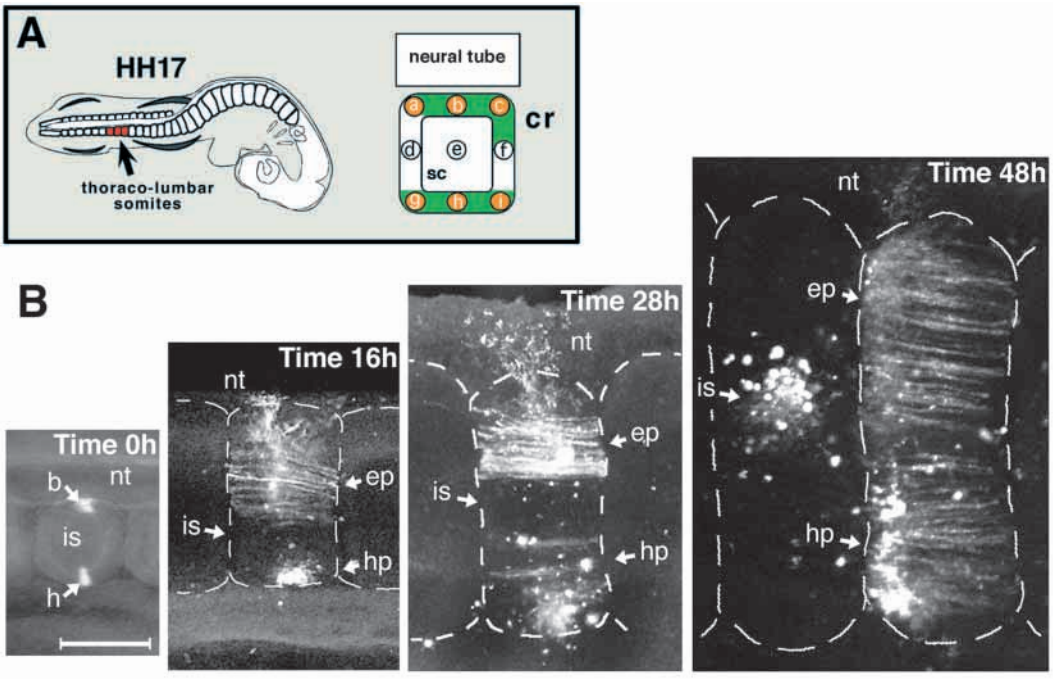

Fig. 1. Early epaxial and hypaxial myotomes expand in opposite dorso-medial and ventrolateral directions, respectively. (A) A dorsal view of the chicken embryo showing targeted thoraco-lumbar somites (red) for dye labeling in chicken embryos between HH15-17, and an enlarged dorsal view of a dermomyotome (between somite stages 4-9) with dye-labeling sites in the dorsomedial (sites a, b, c) and ventrolateral (sites g, h, i) lips. Myotome precursor cells within these sites (green color) are the source of early epaxial and hypaxial myotome fibers. (B) A series showing the development of the early epaxial and hypaxial myotome over 2 days. 0 hour: dermomyotome dye labeling at sites b and h (0 hour, 16 hours and 28 hours) illustrates three dermomyotome regions — a dye-labeled dorsomedial lip, an unlabeled intervening space (site e), and a dye-labeled ventrolateral lip. 16 hour: epaxial myotome growth is occurring, but hypaxial myotome growth is delayed. Also, the unlabeled intervening space is well delimited. 28 hour: this marks the first clear expression of hypaxial myotome growth. At this time, the growth of the epaxial and hypaxial myotomes is simultaneously underway, and the unlabeled intervening space is clearly identifiable between the two myotome domains. 48 hour: a pair of somites from a 28 somite embryo, dye labeled at site e (stage 6) or at sites a and g (stage 7), and re-incubated for 48 hours. No dye-labeled myotome fibers resulted from the site e injection and dye-labeled dermomyotome cells remained clustered. Dye-labeled myotome fibers resulting from injections at sites a and g are broadly distributed along the mediolateral axis of the myotome and individual dye-labeled dermomyotome cells are superimposed showing that mediolateral expansion is due primarily to growth from the dermomyotome dorsomedial and ventrolateral lips. Somite boundaries are marked by dashed lines. Scale bar 250 μm. nt, neural tube; ep, epaxial domain; is, intervening space; hp, hypaxial domain; sc, somitocoel; cr, cranial (cranial direction is to the right in all panels).

In this paper, a similar site-specific dye-labeling strategy was used to analyze hypaxial myotome formation in thoraco-lumbar level somites (somites 21-25, numbered cranial-to-caudal) of HH15-17 chicken embryos (Fig. 1A). A typical example of dye micro-injections made in the dorsomedial and ventrolateral lips of the dermomyotome is shown (Fig. 1B; Time 0 hours, sites b and h). Dye delivery was focal and did not extend into other regions of the dermomyotome sheet allowing the observation of both the early epaxial and hypaxial myotome development simultaneously. The development of epaxial and hypaxial myotome fibers from dermomyotome cells was then followed by confocal imaging of nascent myotome fibers at 16, 28 and 48 hour intervals (Fig. 1B).

In wingbud level somites, a high incidence of epaxial myotome fiber labeling was found after injections along the dorsomedial and craniomedial lips of the dermomyotome. Injections at similar sites in thoracic somite dermomyotomes also gave a high incidence of epaxial myotome labeling after 16-20 hours of embryo re-incubation (Fig. 1B; 16 hours). The epaxial myotome fibers completely spanned the cranio-caudal somite axis at more lateral positions. By contrast, despite strong dye-labeling at sites along the ventral dermomyotome lip, there was either no hypaxial myotome fiber growth, or only a few spindle-like cells in the hypaxial myotome region and none of these cells were observed to span the somite cranio-caudal axis. By HH21 (Fig. 1B; 28 hours), a few labeled hypaxial myotome fibers completely spanned the cranio-caudal somite axis but the density of labeled hypaxial myotome fibers was much less than that observed in the epaxial myotome. These observations suggested that the development of the hypaxial myotome lagged behind that of the epaxial myotome in thoraco-lumbar somites.

By HH26 (Fig. 1B; 48 hours), however, there is considerable mediolateral expansion in both the epaxial and hypaxial domains as revealed by the growth of the somite dermomyotome as well as the extensive distribution of dye-labeled myotome fibers. The growth of the epaxial myotome continued to increase dorsally, showing many full-length, highly organized fibers. Likewise, the hypaxial myotome showed an equally large ventrolateral expansion that consisted of highly organized fibers spanning the cranio-caudal width of the somite. Finally, cells labeled within the dermomyotome intervening space region (Fig. 1B; 48 hours) neither expanded to a comparable degree nor gave rise to myotome fibers between HH19 and HH21, although desmin and myosin heavy chain antibody labeling shows that myotome fibers are located beneath this region at these later stages of somite development (see below).

Because the epaxial and hypaxial myotomes expand respectively in dorsomedial and ventrolateral directions, but remain separated by an unlabeled region in the central somite, we hypothesize that epaxial and hypaxial myotome growth occurs in opposite directions. If true, then early fiber growth patterns should be inverted in the hypaxial domain as compared to that of the epaxial domain. To test this hypothesis, dye

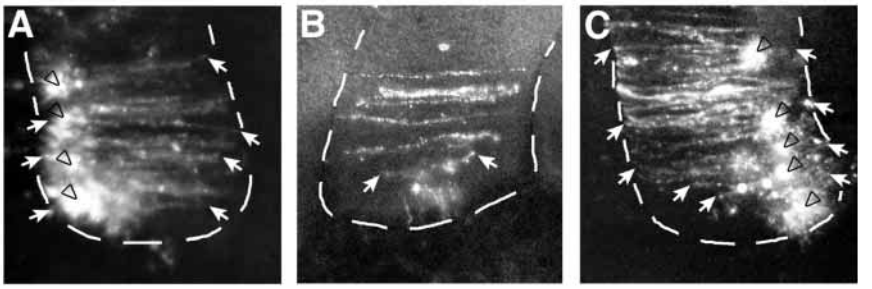

Fig. 2. The early expansion of dye-labeled hypaxial myotome fibers shows that it is growing in a ventrolateral direction. High magnification images of thoraco-lumbar level somites showing hypaxial myotome formation after more than 28 hours of embryo growth. (A-C) Examples of hypaxial myotome growth seen by dye injections over the entire dermomyotome ventrolateral lip: (A) site g; (B) site h, and (C) site i. In all cases, large, full-length, myotome fibers occur at medial locations in the hypaxial myotome while at more lateral positions, myotome fibers are shorter and do not span the cranio-caudal somite axis. These fibers become progressively shorter near the ventrolateral lip (arrows) illustrating their younger age in the somite (see text). The trail of dermomyotome cells labeled from the initial site of dye labeling in the ventrolateral dermomyotome lip is evident (open arrowheads) and myotome fiber lengths are shown extending beyond these bright areas and inserting into the cranial and caudal somite borders (arrows). The somite boundary is marked by a dashed line.

injections were made at 3 sites (g, h and i) along the ventrolateral dermomyotome lip and then analyzed after 24-36 hours of embryo re-incubation to catch nascent hypaxial myotome fibers during elongation (Fig. 2). When sites g and i were injected, dye-labeled myotome fibers were full-length medially and progressively shorter laterally at the caudal or cranial extreme, respectively (Fig. 2A,C). Similarly, after injection at site h, nascent myotome fibers were also shorter laterally but the myotome fiber tips did not extend to either the cranial or caudal somite border (Fig. 2B). Because shorter myotome fibers are younger (Denetclaw et al., 1997) these results confirm that the hypaxial myotome forms in a medial to lateral direction, a pattern inverted as compared to that of the epaxial myotome. The orientation of the growing myotome fiber tips relative to the site of injection also suggests that after myotomal myocytes translocate into the myotome layer from either the dorsomedial or ventrolateral dermomyotome lips, they initiate elongation without additional translocations in either cranio-caudal or mediolateral directions. Thus, in the chicken thoraco-lumbar somite, epaxial and hypaxial myotomes form through a similar mechanistic process, except that myotome formation proceeds in opposite dorsal-ward and ventral-ward directions, respectively.

Quantitation of somite growth and development of the epaxial and hypaxial somite domains

Dye injections in the medial and lateral dermomyotome lips of thoraco-lumbar somites show that the progressive dye-labeled cell expansions that occur in the epaxial and hypaxial myotome are coincident with corresponding increases in the mediolateral axis of the somite dermomyotome (Fig. 3A). Table 1 lists the dimensions of components of the myotome and dermomyotome of thoraco-lumbar somites at various stages of development. Fig. 3B shows that the dermomyotome area increases more than threefold by 24 hours and more than eightfold by 48 hours. The large increase in mediolateral axis growth may be defined by differences in rates of growth in the epaxial and hypaxial somite domains (Fig. 3C). Table 2 shows a breakdown of the thoraco-lumbar somite growth rate, including rates for epaxial, hypaxial, and intervening space areas, based on the expansion of dye-labeled, and unlabeled, cells in the dermomyotome and myotome layers over 1 day (HH20-23) or 2 days (HH25-26) of embryo growth. At HH20-23, the epaxial domain exhibited a significantly greater rate of growth than the hypaxial domain (P=0.0024). By HH25-26, however, the growth rate for the hypaxial domain increased to match that of the epaxial domain growth rates and was no longer significantly different (P=0.1763). The intervening space region was a minor contributor to the overall size increase in the mediolateral somite axis consistent with our observation by dye injections in the dermomyotome sheet (site e) where dye-labeled cells remained localized around the injection site (Fig. 1B; Time 48 hours).

A comparison of epaxial domain growth rates between

Table 1. Measurements of the thoraco-lumbar somite dermomyotome following dye-labeling and embryo growth

Embryo growth (hours)*	Measurements (μm)¶				
	Cranio-caudal axis‡	Medio-lateral axis‡	Epaxial domain§	Intervening space§	Hypaxial domain§
HH15-17 (0)	221±15 *n*=11	225±28 *n*=11	35±8 *n*=8	143±32 *n*=8	44±13 *n*=8
HH18-19 (10-20)	262±22 *n*=6	479±72 *n*=6	236±129 *n*=3	108±49 *n*=3	162±7 *n*=3
HH20-23 (21-30)	311±33 *n*=21	591±83 *n*=21	271±68 *n*=15	124±65 *n*=14	204±60 *n*=16
HH25-26 (41-50)	377±41 *n*=14	1110±92 *n*=14	497±101 *n*=14	140±47 *n*=13	465±75 *n*=14

*Chicken embryo age according to Hamburger and Hamilton (1951) staging and hours of growth after dye labeling (in parentheses).

‡Measurements of somite dermomyotome dimensions based on direct measurements of somite boundaries.

§Measurements of epaxial, hypaxial and intervening space domains based on dye distribution following labeling of dermomyotome dorso-medial and ventro-lateral lips and embryo growth for the indicated times. The intervening space is the unlabeled dermomyotome region between the dye injected dermomyotome lips.

¶Measurements in micrometers given as mean±s.d.; *n*, number of samples.

Table 2. Dermomyotome growth rates in thoraco-lumbar somites

	Measurements (μm/hr)¶					*t*-test§		
Embryo growth (hours)*	Cranio-caudal axis	Medio-lateral axis‡	Epaxial domain‡	Intervening space‡	Hypaxial domain‡	Epaxial vs hypaxial	Epaxial vs epaxial	Hypaxial vs hypaxial
HH20-23 (21-30)	3.6±1.4 *n*=20	14.8±3.0 *n*=20	9.7±3.1 *n*=15	–0.91±2.6 *n*=14	6.6±2.4 *n*=15	*P*<0.01 significant	–	–
HH 25-26 (41-50)	3.9±1.7 *n*=12	25.3±6.7 *n*=14	10.1±2.3 *n*=14	0.17±1.2 *n*=14	9.2±1.6 *n*=14	*P*>0.1 not significant	*P*>0.1 not significant	*P*<0.01 significant

*Chicken embryo age according to Hamburger and Hamilton (1951) staging and hours of growth after dye labeling (in parentheses).
‡Growth rates for epaxial, hypaxial and intervening space regions based on distribution of dye-labeled dermomyotome and myotome cells in each region (see Materials and Methods).
§Statistical analysis of growth rates using a one-tailed, student's *t*-test, significance was $P \leq 0.05$.
¶Measurements in micrometers/hour given as mean±s.d.; *n*=number of samples.

HH20-23 and HH25-26 shows that the two rates are statistically the same (P=0.2084) indicating that growth in the epaxial domain may be proceeding at a maximum rate. A further comparison of hypaxial domain growth rates over this same 2 day period shows that hypaxial domain growth was significantly greater at HH25-26 (P<0.0001) (see Table 2). Because the hypaxial domain growth rate at HH25-26 is essentially equal to the epaxial domain growth rate at HH20-23 and HH25-26, this suggests that both may be proceeding at a maximal rate. If correct, then the initial exponential rate of expansion of the dermomyotome mediolateral axis can be expected to become linear with longer embryo incubation times. In addition to the measured somite domain growth rates, a clear difference in overall dermomyotome growth rates was found between HH20-23 and HH25-26 in the cranio-caudal axis: 3.6±1.4 μm/hour and 3.9±1.7 μm/hour, and in the mediolateral axis: 14.8±3.0 μm/hour and 25.3±6.7 μm/hour, respectively (Fig. 3C). The increase in cranio-caudal growth rate was not statistically significant (P=0.2960), whereas the increase in mediolateral growth rate was highly significant (P<0.0001).

Myotome fiber age and localized expression of contractile proteins

As indicated above and elsewhere (Denetclaw et al., 1997), the oldest myotome fibers are laterally located in the epaxial myotome and medially located in the hypaxial myotome. Fluorescently labeled fibers resulting from injection at site b at stage 8 of thoraco-lumbar somite development are therefore located close to the extreme ventrolateral limit of the epaxial domain. To further analyze the relative position of such fibers, embryos (HH15-17) in which a thoraco-lumbar somite had been injected at site b, were incubated overnight, sectioned in the transverse plane and stained with antibodies to desmin (Fig. 4A-C), a contractile protein known to be expressed by all myotome fibers, including the earliest, nascent myocytes (Kaehn et al., 1988). As predicted, the dye-labeled fibers lie close to the epaxial-hypaxial margin in cross section (dotted line, Fig. 4B,C). In addition, the lateral-to-medial trail of dye-labeled myotome cells can be seen to occupy a relatively superficial position in the myotome, indicating that appositional growth (defined here as growth in the superficial-to-deep plane) in early myotome development involves addition of newer fibers subjacent to existing fibers.

To provide an independent measure of myotome fiber age, we next analyzed the position of fibers that stain with antibodies against the contractile protein myosin heavy chain which is known to appear subsequent to the appearance of desmin protein during early muscle development (Lin et al., 1994). Myosin-expressing myotome fibers were also superficially restricted, both in the epaxial myotome and in the medial-most region of the hypaxial myotome (Fig. 4D-F). C-protein expression is activated after myosin heavy chain has already been activated during primary myocyte differentiation in vitro (Lin et al., 1994). C-protein antibodies also stained the most superficial fibers of the myotome, whether viewed in transverse section (Fig. 4G,H) or coronal section (Fig. 4I). These results support a view of myotome development in which myotome fiber age varies according to two axes. The oldest fibers mark the original position of the somite, and growth in the epaxial domain occurs first in a dorsomedial direction as new fibers are deposited medially and subsequently in a superficial-to-deep direction as new fibers are deposited in layers subjacent to existing myotome fibers. These observations are also consistent with the previous conclusions of Kalcheim and coworkers (Kahane et al., 1998) that newer fibers occupy a deeper position at later stages of myotome development.

The source, however, for the precursor cells in this deeper layer of the myotome is less well understood. Kalcheim and coworkers suggest that these, and indeed all cells, of the myotome arise from precursor cells located in either the cranial or caudal dermomyotome lips (Kahane et al., 1998). Double dye injection experiments, on the other hand, indicate that while the cranial and caudal lips do contribute to deep myotome formation their contribution is consistently quantitatively less than that obtained after injection of either the dorso-medial and ventro-lateral lips (Fig. 5A-F). Figure 5G-I also shows an experiment in which deep medial cells were injected with DiI while simultaneously injecting superficial medial cells with DiO. DiO-labeled fibers are located in a more lateral (older) position in the myotome indicating their earlier birthdate (n=5). Furthermore, when a deep medial DiI injection is coupled with superficial DiO labeling at the somite cranio-medial corner, DiO-labeled fibers are located all along the medio-lateral extent of the epaxial myotome (Fig. 5J-L) whereas the few fibers detected from the deep medial injection do not (n=8). The DiO-labeled fibers in the extreme lateral position correspond, therefore, to the earliest differentiated myotome cells noted by Christ and coworkers (Kaehn et al., 1988) to be born beneath the cranio-medial corner of the dermomyotome. No DiI-labeled fibers are seen in this position

as would be expected if cells from the deep medial position had translocated to populate the entire medio-lateral extent of the cranial dermomyotome lip prior to initiating myotome cell differentiation as predicted elsewhere. Therefore, the earliest myotome fibers located in the extreme lateral position of the epaxial myotome are one and the same as the earliest nascent myocytes identified by Christ and coworkers directly subjacent to the cranio-medial corner of the dermomyotome. The precursor-product analysis presented here and elsewhere indicate that these first myotome cells arise from precursor cells located in the same relative position in the dermomyotome epithelium.

DISCUSSION

Cellular and molecular events in myotome formation

The issue of somitic myotome formation has been a topic of speculation for more than a century (reviewed by Ede and El-Gadi, 1986) and several

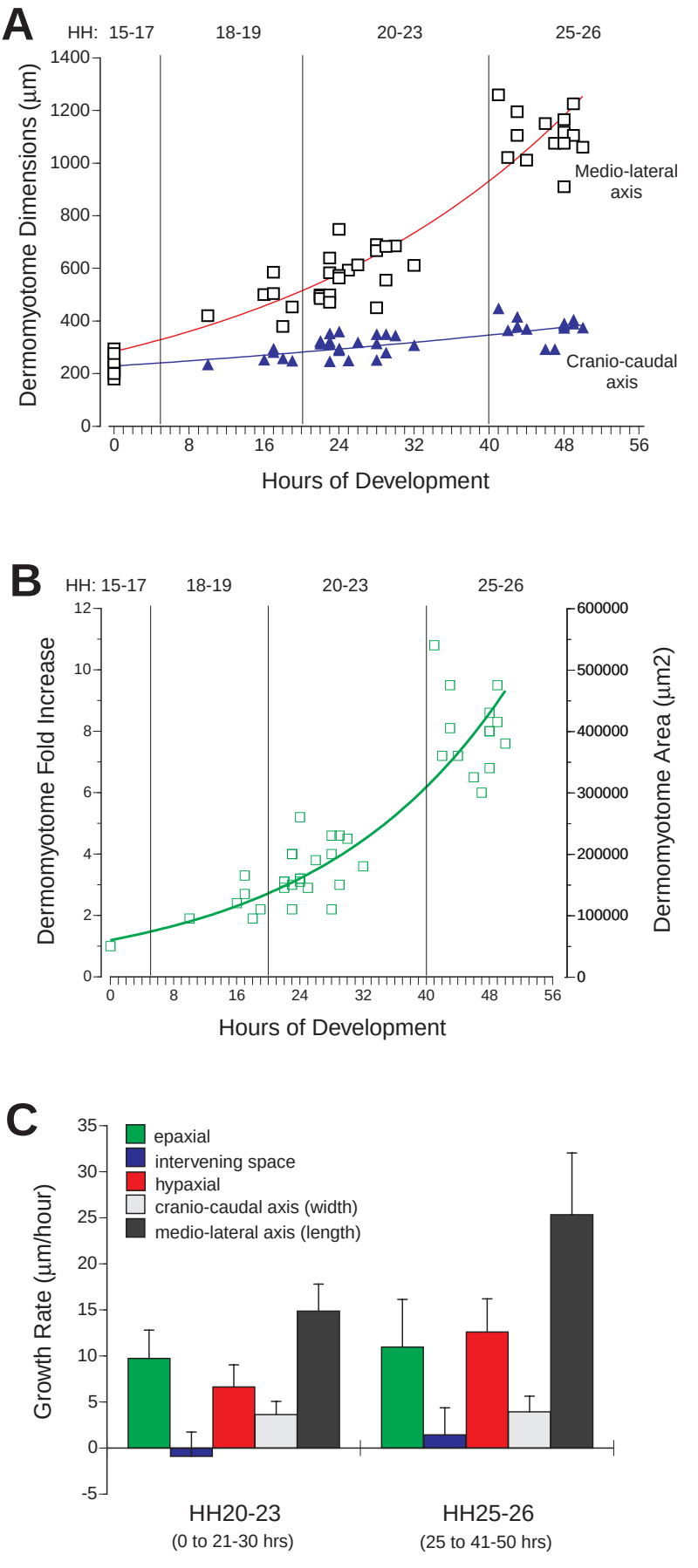

Fig. 3. Quantitative analysis of early dermomyotome and myotome growth in thoraco-lumbar somites. (A) The dermomyotomes of thoraco-lumbar somites, in embryos between HH15-17, are initially equal in size in both cranio-caudal and mediolateral axes (time 0), but show progressive increases in size after overnight to 2 days of embryo growth. The dermomyotome showed a small but gradual increase in size in its cranio-caudal axis (blue line), in contrast, growth of its mediolateral axis (red line) was large over the 2 additional days of embryo incubation. (B) Dermomyotome area showing change in size expressed as either fold-increase or as calculated values (μm^2). Curve fitting regression analysis indicates an initial exponential rate of growth (R^2=0.87) for dermomyotome fold-increase at early stages of thoraco-lumbar somite development. The fold-increase in dermomyotome area was calculated by multiplying dermomyotome width and length at the end of embryo growth periods and dividing by the average dermomyotome area value at time 0. (C.) Comparison of dermomyotome epaxial and hypaxial domain growth rates in embryos at HH20-23 and HH25-26 (see Methods for details). At HH20-23, the rate of epaxial growth is significantly greater than the rate of hypaxial domain growth (P=0.0024). However, at HH25-26, no significant difference in growth rate occurs between these same domains (P=0.1763). Furthermore, a comparison of epaxial domain and hypaxial domain growth rates between HH20-23 and HH25-26 shows that the epaxial domain growth rate is unchanged (P=0.2084), although a significant increase (P<0.0001) is found in the hypaxial domain growth rate at HH25-26. Dermomyotome intervening space growth rates show only a small, non-significant change (P=0.3240) over these same embryo stages. Furthermore, a comparison of the cranio-caudal and mediolateral axis growth rates at HH20-23 and HH25-26 shows that the differences in growth rates are extremely significant (P<0.0001), whereas at time 0, no difference in size occurs along these same axes. Table 2 contains growth rate values for thoraco-lumbar somites.

approaches have been used to understand the earliest events in embryonic myogenesis. The observation that after long-term incubation of embryos with [^{3}H]thymidine, cells with radiolabeled nuclei were located throughout the dermomyotome layer and superimposed above [^{3}H]thymidine-labeled myotome fibers, led to the conclusion that myotome progenitor cells come from the whole dermomyotome and myotome fiber growth begins by simple and direct translocation to the subjacent myotome layer (Langman and Nelson, 1968). In a more recent model of myotome formation (Kaehn et al., 1988), Christ and coworkers suggested that the dermomyotome cranial lip is the source of myotome precursor cells based, in part, upon the triangular shape of the desmin staining pattern of the lateral-most extent of the myotome. This same triangular arrangement of the lateral-most epaxial myotome fibers can also be seen in embryo whole mount assays using muscle protein antibodies (Holtzer et al., 1957; Borman and Yorde, 1994) and cRNA probes for the mRNAs of muscle determination factors (MDFs) (de la Brousse and Emerson, 1990; Ott et al., 1991; Pownall and Emerson, 1992). The process of somitic skeletal myogenesis is dependent on the expression of MDFs including *myoD* and the related basic helix-loop-helix gene transcription factors *myf-5*, *MRF4* and *myogenin* (MDFs are also collectively referred to as muscle regulatory factors (MRFs) (Buckingham, 1992). Antibodies to *myf-5*, the first MDF expressed in the mouse embryo, initially label cells at the somite dorso-medial-cranial corner; then along the whole cranio-caudal somite axis at the dorso-medial lip (Smith et al., 1994). In avian embryos, the presumptive *myoD* iso-mRNA is expressed in a temporal and spatial pattern similar to that of *myf-5* in the mouse. Neither of the myotome development models outlined above can explain the role of the MDF-positive cells within the dorso-medial lip of the somite dermomyotome.

Dye-labeling studies to fate map the dermomyotome (Denetclaw et al., 1997) established a precursor-product relationship between the MDF-positive cells in the dermomyotome dorso-medial lip and early epaxial myotome fibers. Epaxial myotome fibers are the first differentiated skeletal myocytes to appear within each somite and in the embryonic development of birds and mammals (Ordahl and Williams, 1998). The experiments reported here demonstrate

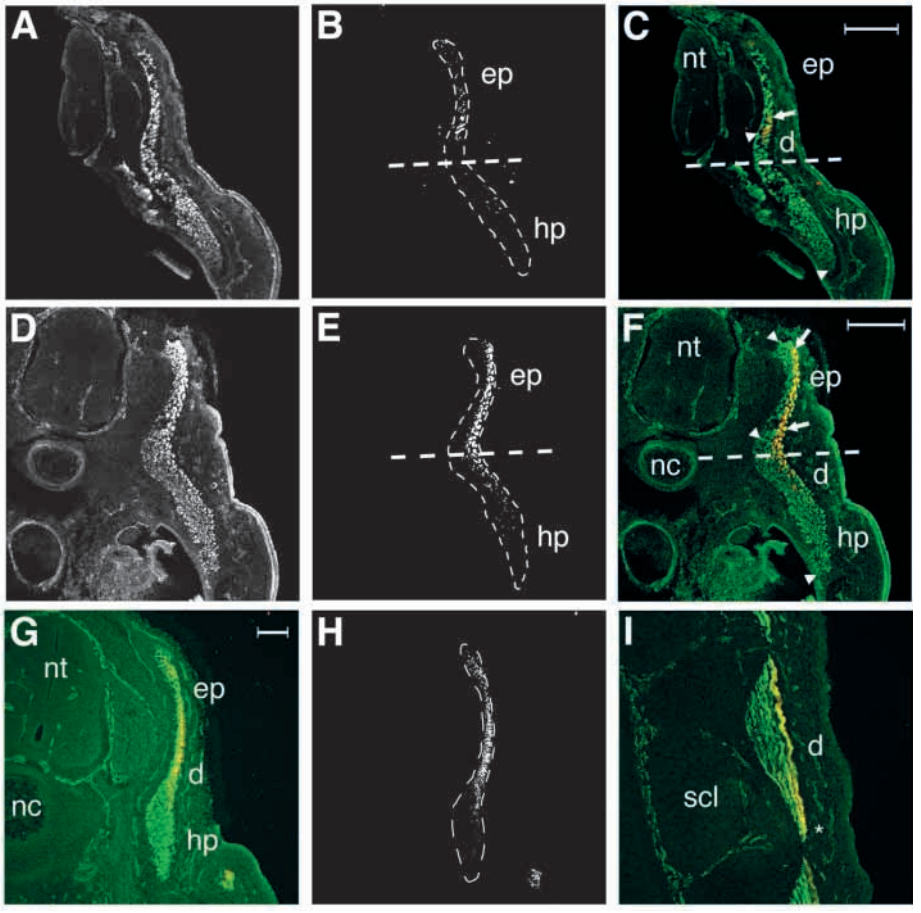

Fig. 4. Dye and antibody labeling of early and late myotome fibers. (A-C) Cross section of a thoraco-lumbar somite showing desmin antibody and DiI labeled myotome fibers. (A) Desmin antibody labels the entire myotome layer. (B) Myotome fibers labeled with DiI are contained in the desmin-labeled myotome (outlined by dashed lines). (C) A false-color image from overlaid desmin (green) and DiI (red) image panels revealing that DiI-labeled myotome fibers are located at the most superficial position in the myotome layer. These DiI-labeled fibers resulted from a somite stage 8 medial lip injection and therefore represent the oldest myotome fibers in the epaxial myotome domain. In B and C, a straight dashed line marks the separation of the epaxial and hypaxial myotome domains as demarcated by DiI-labeled myotome fibers. (D-F) Antibodies to early (desmin) and later (myosin heavy chain) expressed muscle contractile proteins label discrete myotome areas in a cross section of a thoraco-lumbar somite from an HH25 chicken embryos. (D) Desmin antibody labeling of the myotome layer. (E) Myosin heavy chain labeling of a subpopulation of myotome fibers in the myotome layer (outlined by a dashed line). (F) False-color image showing myotome fibers expressing desmin (green) and myosin heavy chain (red) proteins and their co-localization (arrows) in the myotome layer (yellow). Myotome fibers expressing myosin heavy chain were located superficially in the myotome layer (arrows) in contrast to fibers expressing only desmin which were found deep in myotome layer (arrowheads). (G-I) Expression of C-protein, a late expressed muscle contractile protein, in the myotome layer. (G) False-color image showing desmin (green) and C-protein (red) antibody labeling. C-protein-expressing fibers are located superficially within the myotome. (H) A comparison of C-protein expression within the desmin-labeled myotome layer (dashed outline). (I) A false-color coronal image showing that late expressed C-protein is present in only the most superficial myotome fibers which are large in diameter and fully extended across the somite. DiI, myosin heavy chain, and C-protein panels are shown as thresheld images. All panels are composite images produced from confocal serial z-axis sections and are displayed as 8-bit grayscale images or combined to form rgb false-color images. Scale bar 100 μm. nt, neural tube; nc, notochord; d, dermis; ep, epaxial; hp, hypaxial; scl, sclerotome; asterisk, cranial end.

that the cell movements in myotome formation deduced from dye-labeling of wing level somites also occur during formation of the epaxial myotome in thoraco-lumbar somites. The morphological changes in the dermomyotome and epaxial myotome are similar in the somites at all axial levels, with the possible exception of the cranial-most few somites where the cellular movements that lead to muscle formation are less well-described (Huang et al., 1997). We conclude, therefore, that this early phase of epaxial myotome formation is essentially identical in the somites at all axial levels.

The formation of hypaxial musculature, by contrast, varies substantially at different axial levels (Ordahl and Williams, 1998; Dietrich et al., 1998). In brachial somites, for example, cells migrate from the lateral regions of the dermomyotome to the adjacent limb bud, where they intermingle with limb mesenchyme cells derived from the lateral plate (somatic) mesoderm (Christ et al., 1974, 1977; Chevallier et al., 1977; Jacob et al., 1978, 1979). At thoraco-lumbar levels, however, the dermomyotome epithelium elongates ventro-laterally as the hypaxial myotome forms beneath (Straus and Rawles, 1953; Seno, 1961; Christ et al., 1983). A major goal of the present study, therefore, was to compare the development of the hypaxial myotome with that of the epaxial myotome. The results, summarized in Fig. 6, permit the following statements to be made regarding thoraco-lumbar somites. (1) The regions of the dermomyotome most active in the generation of epaxial and hypaxial myotome fibers are, respectively, the dorso-medial and ventro-lateral lips, sites that show early and persistent expression of MDF genes. (2) Myotome growth in epaxial and hypaxial domains progresses through similar mechanisms of cell movement and growth, except that myotome expansion is in opposite dorso-medial and ventro-lateral directions, respectively (Fig. 6B,C). (3) Maximum rate of myotome development is similar in the epaxial and hypaxial domains but the timing of onset and completion of myotome formation differs in each domain (Fig. 3). (4) The slower rate of cranio-caudal expansion of the dermomyotome is initially correlated with a slower rate of development of myotome fibers at the cranial and caudal lips. (5) The appositional growth of the myotome occurs through formation of increasingly deeper layers of myotome fibers (Fig. 4). (6) Myotome development in both epaxial and hypaxial domains is directly correlated with and, we propose, coupled to the corresponding expansion of the overlying dermomyotome epithelium (see below). Thus, once the formation of the epaxial and hypaxial myotome is underway, new myoblast cells are produced along all margins of the somite dermomyotome but at different rates and at different times during development and with time- and position-specific deposition of nascent myofibers within the myotome.

Growth zones in the dermomyotome

The onset of epaxial myotome formation is earlier, relative to somite stage, in lumbosacral versus cervical somites in the avian embryo (Borman and Yorde, 1994). In the thoraco-lumbar somites initiation of hypaxial myotome formation is delayed by about one day relative to that of the epaxial myotome (Fig. 1B). However, once hypaxial myotome formation is underway, the rate of dermomyotome and myotome growth in both domains progresses at similar rates over a 2 day period of embryonic development (Fig. 3C). At subsequent stages of embryo and fetal development changes in these growth rates may modulate the relative amount of medio-lateral versus appositional growth in each body domain.

The most active regions of myotome precursor cell activity in the dermomyotome also correspond to its most active growth fronts. What is the motive force behind this directional expansion of the dermomyotome and myotome? Dye injections into a small population of cells in the dorso-medial and ventro-lateral lips of the dermomyotome results in trails of dye-labeled dermomyotome cells and myotome fibers (see, for example, Fig. 1B; 48 hours, right somite; Fig. 2A,C). By contrast, dye injection into the dermomyotome intervening space region results in few, if any, myotome fibers and a minimal expansion of the dye (Fig. 1B; 48 hours, left somite). These results indicate that the highest rate of cell proliferation in the dermomyotome occurs in or near its dorso-medial and ventro-lateral lips. We hypothesize that these are regions of high level stem cell proliferation (Fig. 6D) that simultaneously produce at least two kinds of daughters. (1) Myotomal myoblast cells that undergo morphogenetic cell movements and leave the dermomyotome to enter the subjacent myotome (mt) layer as nascent myocytes (Fig. 6C, translocation region); and (2) dermomyotome epithelium cells that remain, either as proliferative stem cells or as relatively quiescent dermomyotome cells that are left behind as the growing lip moves medialward (Fig. 6D, growth region). The dynamic instability of the dorso-medial and ventro-lateral dermomyotome lips, which is likely to be a result of adjacent stem cell activity, allows the mitotic expansion of the dermomyotome to proceed directionally with concomitant deposition of nascent myotome fibers in the same direction.

Two additional growth processes may also be implicated in the expansion of the myotome. First, as nascent myotome fibers elongate in the cranio-caudal direction they may generate a convergent-extension type of force (Keller, 1985; Keller et al., 1985) that, because of the regimented cranio-caudal orientation of the myocytes, would be expected to exert pressure within the myotome in a dorso-medial or ventro-lateral direction (Fig. 6E). Second, hypertrophy of fully elongated fibers can be expected to subsequently amplify this force. What might allow these forces to be exerted unidirectionally; eg. in a dorso-medial direction for the epaxial myotome? A definitive answer is not yet available but the ultimate answer is likely to be related to the establishment of a domain boundary between the epaxial and hypaxial domains (dashed line, Fig. 6E). Such a boundary is evident in the behavior of migratory somite cells and the invagination of ectoderm along this boundary at brachial levels (Ordahl and Le Douarin, 1992) and apoptosis along this boundary at later stages of forelimb level somites (Tosney, 1994). The net effect of the divergent growth processes is to help drive expansion and morphogenesis of the epaxial and hypaxial domains of the embryonic body (Fig. 6E).

Mouse embryos bearing mutations of key muscle genes may have disruptions in important steps in the myotome development process. For example, mouse embryos lacking an intact *myf-5* gene fail to form early myotome fibers, but when the *myf-5* gene disruption is accompanied by insertion of a *lacZ* reporter gene to indicate cells in which the *myf-5* locus is transcriptionally active, blue-staining cells appear subjacent to the dermomyotome dorso-medial and ventro-lateral lips

(Tajbakhsh et al., 1996, 1997). Thus, the *myf-5* gene is required for nascent myotomal myoblast cells to execute and complete the myogenic differentiation program but is not required for precursor cell translocation. Therefore, by the time myogenic precursor cells in the dorso-medial lips of the mouse dermomyotome have activated the *myf-5* locus they have already initiated myogenic differentiation and are destined to translocate to the myotome layer. The mechanism(s) that drive myotome precursor cell translocation from the dermomyotome into the myotome layer are unknown, but may require a combination of the expression of specific extracellular matrix proteins (Tosney et al., 1994; Itoh et al., 1994), the expression of appropriate ligand and receptor molecules (Marcelle et al., 1997) and, finally, the overgrowth by the dermomyotome which is known to be mitotically active (Christ and Ordahl, 1995; Amthor et al., 1999). Interestingly, myf-5 null embryos do show dorso-medial to ventro-lateral expansion of the dermomyotome indicating that the *myf-5* gene is not necessary for the mitotic expansion within the dermomyotome epithelium possibly including, therefore, the myogenic stem cells located adjacent to the dorso-medial lip.

These findings highlight issues regarding the effects that

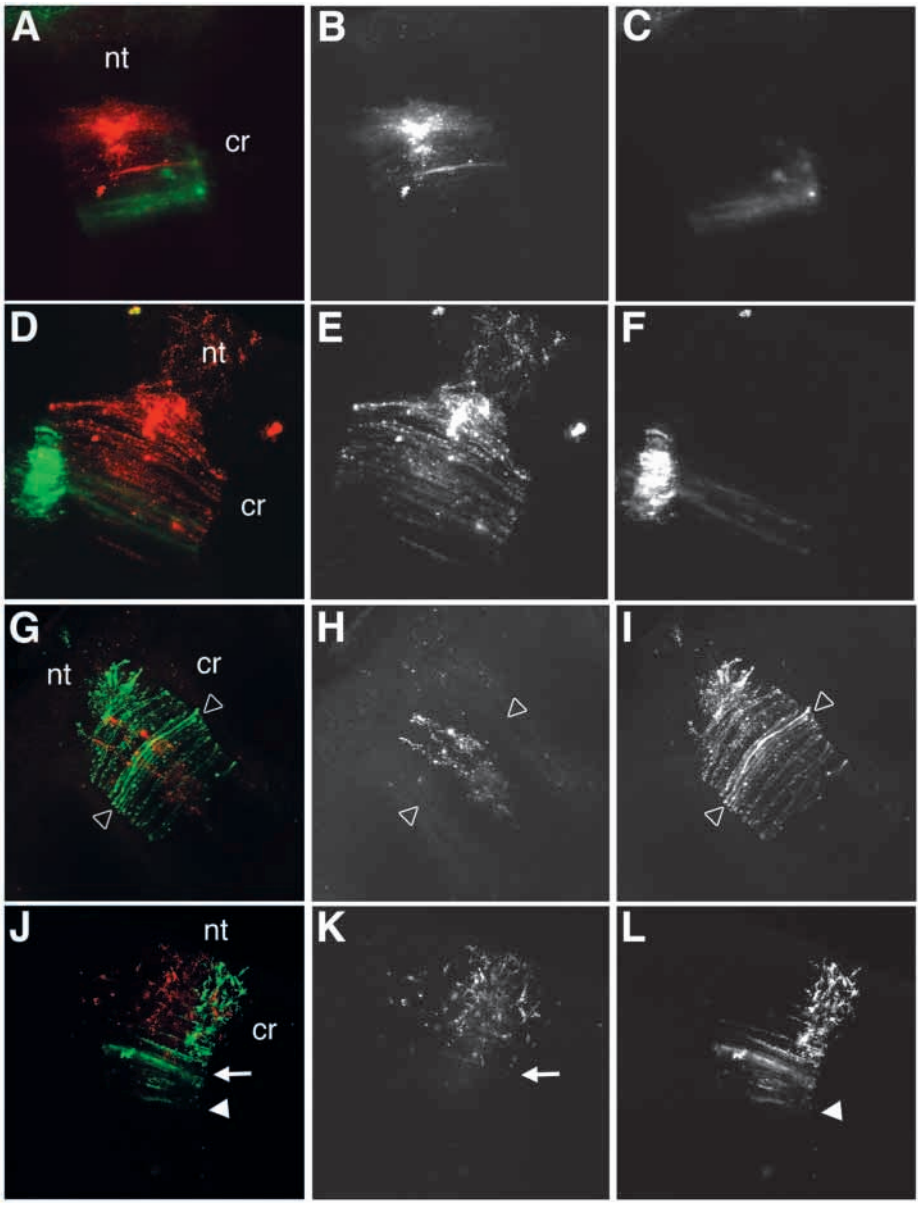

Fig. 5. Dye-labeling and precursor-product analysis of myotome fibers produced from the dermomyotome cranial and caudal lips. (A-F) Embryos with 27 and 30 somites were double-injected in somite stage 7 initially with DiI (dorsomedial, site b) and 6-8 hours later with DiO in the medio-caudal or medio-cranial dermomyotome lip. (A-C) A dorsomedial and mediocranial injection and myotome fiber labeling after overnight embryo growth. (A) False-color image constructed from grayscale DiI (B) and DiO (C) labeled cells. (D-F) Dorsomedial and mediocaudal dye injections and labeled myotome fibers after overnight embryo growth. (D) False-color image constructed from grayscale diI (E) and diO (F) labeled cells. Myotome fibers that result from injections at the dorsomedial lip show a dorsomedial ward expansion consistent with previous findings (Denetclaw et al., 1997). However, injections in mediocranial or mediocaudal dermomyotome borders resulted in few dye-labeled myotome fibers and those fibers that did form were found deep in the myotome layer. (G-L) Embryos (20-28 somites) were also double-injected in somite stages 2-4 with DiI in the medial face of the epithelial somite adjacent to the neural tube (site of proposed myotomal pioneer cells; Kahane et al., 1998) and with DiO in the dorsal epithelium (that is, site b or c in the dermomyotome of older somites). (G-I) Dye labeling of a 25 somite embryo in somite stage 3 with DiI (red) injected in the medial somite epithelium and DiO (green) injected in the dorsomedial epithelium (site b) and grown for 17.5 hours. (G) A false-color image constructed from grayscale DiI (H) and DiO (I) labeled cells. Open arrowheads show the cranial and caudal borders of the somite. (J-L) Dye labeling of a 26 somite embryo in somite stage 3 with DiI (red) injected in the medial somite epithelium and DiO (green) injected in the dorsomedial cranial corner (site c) and grown for 21.5 hours. (J) False-color image constructed from grayscale DiI (K) and DiO (L) labeled cells. Injections in the dorsomedial epithelium (site b or c) resulted in extensive epaxial myotome fiber labeling that included fibers in the extreme lateral-most extent of the epaxial myotome (arrowhead in L) that are labeled Kaehn fibers in Fig. 6. By contrast, injections in the medial face primarily labeled sclerotome (K). Although faint labeling of two fibers was also observed, these labeled fibers were always located more medial to fibers resulting from the corresponding dorsomedial epithelium injections. In no instance did fibers resulting from such medial face injections extend over the full mediolateral somite axis (n=14). Arrows in J and K show the most lateral extent of labeled fibers resulting from a medial face injection, and arrowheads (J,L) show the lateralmost extent of labeled fibers from injections in the dorsomedial epithelium. nt, neural tube; cr, cranial.

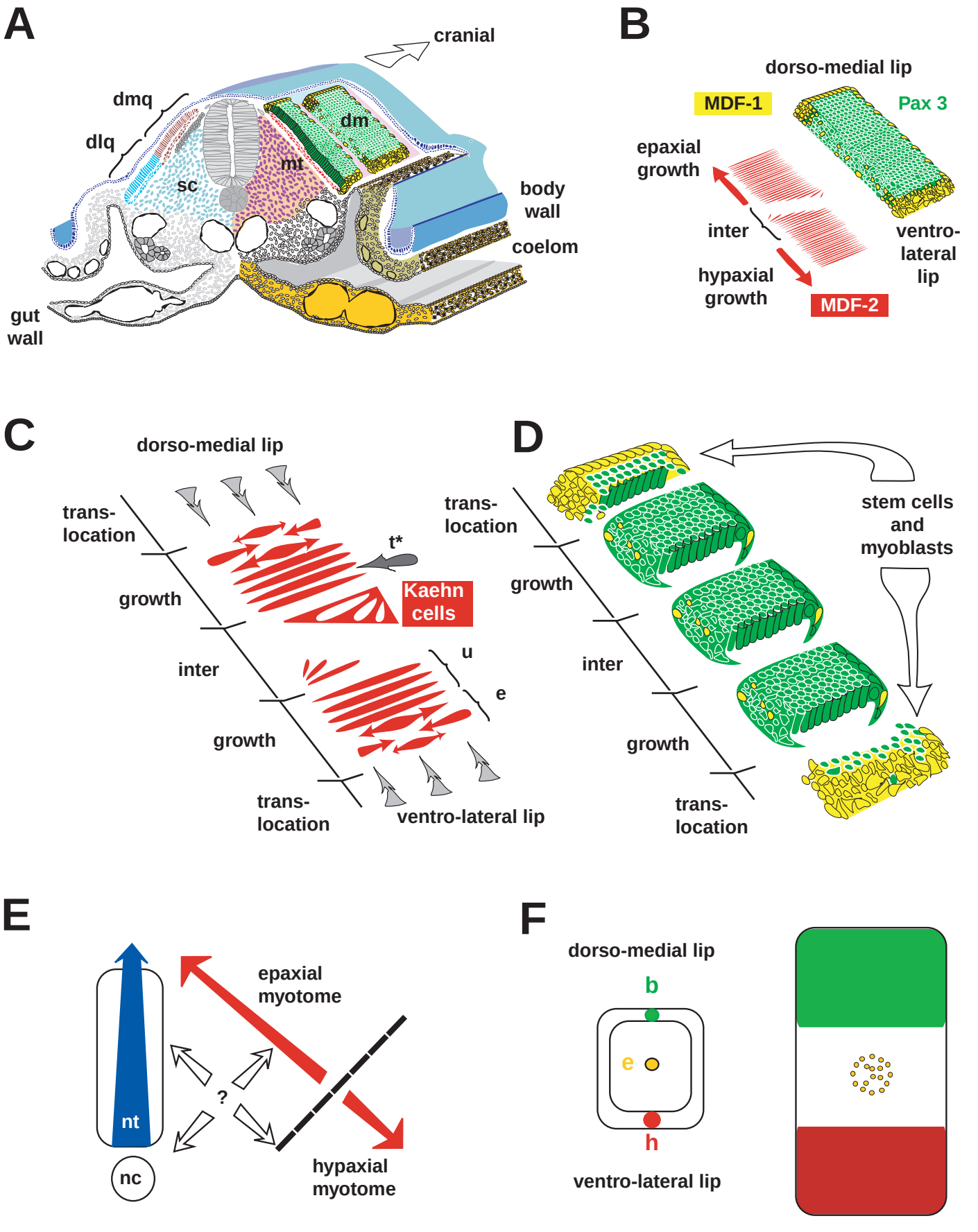
A
cranial
dmq
dlq
dm
mt
sc
body wall
coelom
gut wall
B
dorso-medial lip
MDF-1
Pax 3
epaxial growth
inter
hypaxial growth
MDF-2
ventro-lateral lip
C
dorso-medial lip
trans-location
t*
growth
Kaehn cells
inter
u
e
growth
trans-location
ventro-lateral lip
D
trans-location
stem cells and myoblasts
growth
inter
growth
trans-location
E
epaxial myotome
nt
?
nc
hypaxial myotome
F
dorso-medial lip
b
e
h
ventro-lateral lip

Fig. 6. Summary of early epaxial and hypaxial myotome morphogenesis in thoraco-lumbar somites of the avian embryo. (A) Overview of a somite stage 13 thoraco-lumbar somite showing dorsomedial (dmq) and dorsolateral (dlq) somite quadrants corresponding to dermomyotome precursor cell pools for the epaxial (light brown) and hypaxial (aqua) myotome domains, on the left-hand side. On the right hand side, green represents *Pax-3*-expressing cells of the dermomyotome; yellow, MDF-1-expressing myotome precursor cells concentrated in the lip regions of the dermomyotome, principally the dorsomedial and ventrolateral lips; purple, sclerotome; red, myotome; blue, ectoderm. (B) A higher magnification of the dermomyotome and myotome layers of the somite shown in A. Red arrows show the dorsomedial and ventrolateral expansion directions of the epaxial and hypaxial myotome domains, respectively. MDF2 (red color) indicates that gene expression has progressed past expression of a single MDF and includes additional/alternative MDFs as well as contractile and other muscle-specific proteins. (C) Schematic view of the myotome layer illustrating 5 myotome fiber growth zones in the thoraco-lumbar somite. The growth zone for the hypaxial myotome consists of medially positioned (older) unit-length fibers (u) fully expanded across the cranial-caudal axis of the somite, and shorter (younger) laterally located fibers in the process of elongating across the somite (e) (direction of elongation shown by arrowheads on nascent fibers) after having translocated from the dermomyotome lip (gray arrows). In the case of epaxial myotome development, the opposite arrangements of myotome fibers occurs where older fibers are lateral and younger fibers are more medial in the somite. The translocation zone represents the dorsomedial and ventrolateral extremes of the myotome layer where nascent myocytes arrive in the myotome layer by translocation from all sites along the cranio-caudal axis of the overlying dermomyotome. The large numbers of myocytes entering the myotome at the dorsomedial and ventrolateral locations and their subsequent parallel elongation in the somite by a convergent-extension process and by growth of the myotome fibers may provide a reason for the mediolateral expansion of the myotome. By contrast, the contribution of myotome fibers from the cranial and caudal borders (dark gray arrow labeled t*) is much more limited and is found to add myotome fibers in deeper positions within the myotome. The inter zone identifies the boundary between the epaxial and hypaxial myotomes. The inter zone region contains the first somitic myotome fibers (oldest) identified by Kaehn and Christ (1988) and we propose that an equivalent group of myotome fibers exists for the hypaxial myotome domain. Other contributors to the myotome fiber growth in this inter zone region are presently unknown. (D) The dermomyotome (green) with a zone of heavy stem cell activity in the dorsomedial and ventrolateral lips where myotome precursor cell translocation to the myotome layer occurs. Growth zones in the dermomyotome contain daughters of cells previously residing in the stem cell zone whose positions correspond to their counterparts within the myotome layer (see also Denetclaw et al., 1997). (E) An illustration of the vectorial growth driving expansion of the epaxial and hypaxial domains of the embryonic body. red, epaxial and hypaxial myotome; blue, neural tube; white, sclerotome expansion. (F) A Mexican flag labeling pattern predicted from the dye injection scheme shown (site b, green; site e, gold; site h, red). The green – white (intervening space) – red sequence can be generated by a variety of injection schemes (a,e,g; c,e,i; for two examples), although the relative size of each color field may vary in some cases. The green, white, red motif of the Mexican flag is also found in the flags of many nations. The face of the cross section in A is adapted from a drawing of a stage 13 thoracic somite in Lillies Development of the Chick (Hamilton, 1952). See Ordahl et al. (1999) for details.

extrinsic signals have upon myotome development at different stages of chick embryo development. Recent work from a variety of laboratories implicates three major signaling sources that affect the differentiation of myocytes from cells in the somite: (1) the dorsal neural tube and superficial epaxial ectoderm; (2) the lateral plate mesoderm; and (3) notochord and floor plate of the neural tube (recently reviewed by Currie and Ingham, 1998). As has been pointed out elsewhere (Teillet and Le Douarin, 1983; Teillet et al., 1998) such signals may have substantial effects upon cell proliferation and survival rather than upon cell determination or differentiation per se. Proliferative signals may be sufficient to trigger the stem cell activity within the zones of the dermomyotome that lead to the generation of differentiative daughters (myoblasts) while simultaneously expanding the dermomyotome epithelium.

The dermomyotome as a morphogenetic field

The ‘morphogenetic field’ concept has been used to explain the power of embryonic tissue systems to self-organize and to influence the development of surrounding tissues (Gilbert et al., 1996). The mechanisms by which morphogenetic fields create, express and maintain the ‘positional information’ inherent in organized tissues remain poorly understood. Early field models postulated that cell fate and position are governed by either morphogenetic cell movements (Holtfreter and Hamburger, 1955) or chemical gradients (Child, 1941, 1946). The notion that cell and tissue morphogenetic movements are the mechanistic basis for the organizing principle inherent in the amphibian chordamesoderm field (Holtfreter and Hamburger, 1955) is now well supported by demonstration of cellular convergent-extension movements (Keller et al., 1985; Keller, 1985) and their potential to generate directional force during tissue expansion (Moore et al., 1995). Concentration gradients of intracellular gene products within the syncytial *Drosophila* embryo have been demonstrated to establish axial polarity and positional information prior to cellularization (Roth et al., 1989; Nüsslein-Volhard and Roth, 1989). Modern versions of an extrinsic diffusion gradient model (Wolpert, 1996) postulate that extracellular gradients of chemical morphogens can produce simple patterns, for example, the simple blue-white-red pattern of the French flag, by imparting cell fate and position values to otherwise naive cells within the field (Wolpert, 1969).

Fig. 6F shows that the green-white-red pattern of the Mexican flag can be established in the early myotome through site-specific colored labeling of cells within the overlying dermomyotome epithelium. In this example, green and red dye-labeling in the early embryonic myotome is established by labeling precursor cells located in the dorso-medial and ventro-lateral lips of the dermomyotome, respectively, that in turn translocate into the myotome layer where they undergo terminal differentiation, including cell elongation and acquisition of differentiated cell properties. Gold dye injected into the intervening space region results in labeled cell spreading but no myotome fibers (Fig. 6F). Therefore, in the dermomyotome field, myotome precursor cells establish the pattern of the myotome as a consequence of their morphogenetic cell movements (stem cell division, translocation, and elongation) rather than through interpretation of an extrinsic gradient of chemical morphogens.

The predictability of the morphogenetic cell movements in the dermomyotome field and myotome also provides a framework for interpreting the sequence of gene expression in specific muscle lineages. As indicated above, *myf-5* is the first

MDF expressed in the dorso-medial quadrant of the newly formed mouse somite (Ott et al., 1991). Dye injection shows that the equivalent cells in bird embryos are destined to form the ventrolateralmost epaxial myotome fibers in fore-limb level regions (Denetclaw et al., 1997) (and this paper). Miller and coworkers (Smith et al., 1994) have shown that *myoD* expression is similarly ventro-laterally localized in the epaxial myotomes of early mouse forelimb level somites (see their Fig. 3) and is superficially localized in maturing thoracic myotomes (see their Fig. 6). A similar pattern of MDF expression was predicted for the earliest myotome fibers in avian forelimb-level somites except that the sequence of MDFs was inverted (Williams and Ordahl, 1994). We propose, therefore, that for these earliest myotome fibers (called Kaehn fibers, after their first discoverer; Kaehn et al., 1988; see Fig. 6C) the gene expression sequence is: *Pax-3* (segmental plate cell) → MDF 1 (*myoD*-chick, *myf-5*-mouse) (dermomyotome dorso-medial lip cell) → MDF 2 (*myf-5*-chick, *myoD*-mouse) (myotomal myocyte). Given the speed with which dorso-medial lip cells enter the myotome (<24 hours), we estimate that they could undergo only one or two mitotic divisions before becoming postmitotic myocytes. Based upon these considerations, we conclude that the MDF 1 expressing cells in the dermomyotome lip are myoblast cells (cells with no or limited mitotic capacity that are destined to differentiate into myocytes). Thus, the genetic program sequence for the Kaehn cells can be written as follows: precursor cell (*Pax-3*) → myoblast (*myoD*) → myocyte (*myf-5*). The program for the equivalent cells in the mouse would invert the expression of MDF 1 and 2 and is consistent with previous observations (Cossu et al., 1996). Early gene expression patterns in the dermomyotome and myotome may yield information regarding the lineage and maturation of other subsets of myotome precursor cells as they emerge from the dermomyotome epithelium. It is interesting to speculate that the timing and nature of the site-specific morphogenetic cell movement and growth patterns discussed here may be related to or under control of those gene products.

In a morphogenetic field '...the histological fate of any part of the field depends upon its topographic relationship to the other parts of the field' (Holtfreter and Hamburger, 1955) and this appears to be true for the dermomyotome. As the epithelium expands in a rectangular shape it maintains potentiality for several cell fates while parsing out differentiated progeny in a position- and time-dependent fashion. The first differentiated cell type to emerge is the unique form of mononucleated myocyte found within the myotome. The appearance of differentiated myocytes along the medial lip of the dermomyotome coincides with dermomyotome growth in the medial direction and involves dynamic morphogenetic cell movements that resemble those involved in gastrulation (Ordahl et al., 1999). Nevertheless, myogenic potential for later-stage myocytes persists unexpressed within the central dermomyotome sheet, and myocytes from this region only appear after 48 hours (data not shown). While detailed information regarding the earliest point at which the dermomyotomal precursors of dermis (Viallet et al., 1998) and cartilage (Aoyama and Asamoto, 1988) acquire their positional information are not yet available, the delay in appearance of these two cell types from the dermomyotome epithelium does demonstrate their time dependency. Therefore, the somite dermomyotome exhibits essential characteristics of a morphogenetic field that: distributes potentiality for muscle, dermis and cartilage; influences the development of surrounding tissues, such as the peripheral nervous system; and also provides an engine of growth within the epaxial and hypaxial domains of the early embryonic body.

We wish to thank Drs Kathryn Tosney and Raymond Keller and our many colleagues for helpful discussions and generously sharing unpublished findings. We also thank laboratory members, especially Mr Eli Berdougo for excellent technical assistance on this project. This work was supported by grants to C. P. O. from the National Institutes of Health (AR44483) and the Muscular Dystrophy Association of America. W. F. D. was partially supported by a NRSA Training Grant T32 HL0773105.

REFERENCES

Amthor, H., Christ, B. and Patel, K. (1999). A molecular mechanism enabling continuous embryonic muscle growth – a balance between proliferation and differentiation. *Development* **126**, 1041-1053.

Aoyama, H. and Asamoto, K. (1988). Determination of somite cells: independence of cell differentiation and morphogenesis. *Development* **104**, 15-28.

Bober, E., Franz, T., Arnold, H. H., Gruss, P. and Tremblay, P. (1994). Pax-3 is required for the development of limb muscles: a possible role for the migration of dermomyotomal muscle progenitor cells. *Development* **120**, 603-612.

Borman, W. H. and Yorde, D. E. (1994). Analysis of chick somite myogenesis by in situ confocal microscopy of desmin expression. *J. Histochem. Cytochem.* **42**, 265-272.

Brand-Saberi, B., Ebensperger, C., Wilting, J., Balling, R. and Christ, B. (1993). The ventralizing effect of the notochord on somite differentiation in chick embryos. *Anat. Embryol.* **188**, 239-245.

Brill, G., Kahane, N., Carmeli, C., von Schack, D., Barde, Y. A. and Kalcheim, C. (1995). Epithelial-mesenchymal conversion of dermatome progenitors requires neural tube-derived signals: characterization of the role of Neurotrophin-3. *Development* **121**, 2583-2594.

Buckingham, M. (1992). Making muscle in mammals. *Trends Genet.* **8**, 144-148.

Chevallier, A., Kieny, M. and Mauger, A. (1977). Limb-somite relationship: origin of the limb musculature. *J. Embryol. Exp. Morphol.* **41**, 245-258.

Child, C. M. (1941). *Patterns and Problems of Development.* Chicago: University of Chicago Press.

Child, C. M. (1946). Organizers in development and the organizer concept. *Physiol. Zool.* **19**, 89-148.

Christ, B., Brand-Saberi, B., Grim, M. and Wilting, J. (1992). Local signalling in dermomyotomal cell type specification. *Anat. Embryol.* **186**, 505-510.

Christ, B., Jacob, H. and Jacob, M. (1974). Uber den ursprung der flugelmuskulature. *Experientia* **30**, 1446-1448.

Christ, B., Jacob, H. J. and Jacob, M. (1977). Experimental analysis of the origin of the wing musculature in avian embryos. *Anat. Embryol.* **150**, 171-186.

Christ, B., Jacob, M. and Jacob, H. J. (1983). On the origin and development of the ventrolateral abdominal muscles in the avian embryo. *Anat. Embryol.* **166**, 87-107.

Christ, B. and Ordahl, C. P. (1995). Early stages of chick somite development. *Anat. Embryol. (Berl)* **191**, 381-396.

Cossu, G., Kelly, R., Tajbakhsh, S., Di Donna, S., Vivarelli, E. and Buckingham, M. (1996). Activation of different myogenic pathways: myf-5 is induced by the neural tube and MyoD by the dorsal ectoderm in mouse paraxial mesoderm. *Development* **122**, 429-437.

Currie, P. and Ingham, P. W. (1998). The generation and interpretation of positional information within the vertebrate myotome. *Mech. Dev.* **73**, 3-21.

de la Brousse, C. F. and Emerson, C. P. (1990). Localized expression of a myogenic regulatory gene, qmf1, in the somite dermatome of avian embryos. *Genes Dev.* **4**, 567-581.

Denetclaw, W. F., Jr., Christ, B. and Ordahl, C. P. (1997). Location and growth of epaxial myotome precursor cells. *Development* **124**, 1601-1610.

Dietrich, S., Schubert, F. R., Healy, C., Sharpe, P. T. and Lumsden, A.

(1998). Specification of the hypaxial musculature. *Development* **125**, 2235-2249.

Dietrich, S., Schubert, F. R. and Lumsden, A. (1997). Control of dorsoventral pattern in the chick paraxial mesoderm. *Development* **124**, 3895-3908.

Ede, D. A. and El-Gadi, A. O. (1986). Genetic modifications of developmental acts in chick and mouse somite development. In *Somites in Developing Embryos* (ed. Bellairs, R., Ede, D. A. and Lash, J. W.), pp. 209-224. New York, London: Plenum Press.

Fan, C.-M., Lee, C. S. and Tessier-Lavigne, M. (1997). A role for WNT proteins in induction of dermomyotome. *Dev. Biol.* **191**, 160-165.

Fan, C.-M. and Tessier-Lavigne, M. (1994). Patterning of mammalian somites by surface ectoderm and notochord: evidence for sclerotome induction by a hedgehog homolog. *Cell* **79**, 1175-1186.

Fischel, A. (1895). Zur entwicklung der ventralen rumpf- und extremitatenmuskulatur der Vogel und Saugetiere. *Morph. Jb.* **23**, 544-561.

Gilbert, S. F., Opitz, J. M. and Raff, R. A. (1996). Resynthesizing evolutionary and developmental biology. *Dev. Biol.* **173**, 357-372.

Goulding, M., Lumsden, A. and Paquette, A. J. (1994). Regulation of Pax-3 expression in the dermomyotome and its role in muscle development. *Development* **120**, 957-971.

Hamburger, V. and Hamilton, H. L. (1951). A series of normal stages in the development of the chick embryo. *J. Morphol.* **88**, 49-92.

Hamilton, H. L. (1952). *Lillie's Development of the Chick. An Introduction to Embryology.* New York: Holt.

Holtfreter, J. and Hamburger, V. (1955). Amphibians. In *Analysis of Development* (ed. B. H. Willier, P. Weiss and V. Hamburger), pp. 230-296. Philadelphia and London: W.B. Saunders Co.

Holtzer, H., Marshall, J. M. and Finck, H. (1957). An analysis of myogenesis by the use of fluorescent antimyosin. *J. Biophys. Biochem. Cytol.* **3**, 705-729.

Huang, R., Zhi, Q., Ordahl, C. P. and Christ, B. (1997). The fate of the first avian somite. *Anat. Embryol.* **195**, 435-449.

Itoh, M., Arai, K. and Uehara, K. (1994). Localization of type IV collagen in the myotome cells during the somite differentiation in the chick embryo. *Dev. Growth Differ.* **36**, 427-435.

Jacob, M., Christ, B. and Jacob, H. (1979). The migration of myogenic cells from the somites into the leg region of avian embryos. *Anat. Embryol.* **157**, 291-309.

Jacob, M., Christ, B. and Jacob, H. J. (1978). On the migration of myogenic stem cells into the prospective wing region of chick embryos. *Anat. Embryol.* **153**, 179-193.

Kaehn, K., Jacob, H. J., Christ, B., Hinrichsen, K. and Poelmann, R. E. (1988). The onset of myotome formation in the chick. *Anat. Embryol.* **177**, 191-201.

Kahane, N., Cinnamon, Y. and Kalcheim, C. (1998). The cellular mechanism by which the dermomyotome contributes to the second wave of myotome development. *Development* **125**, 4259-4271.

Keller, R. E. (1985). The cellular basis of amphibian gastrulation. *Dev. Biol.* **2**, 241-327.

Keller, R. E., Danilchik, M., Gimlich, R. and Shih, J. (1985). The function and mechanism of convergent extension during gastrulation of *Xenopus laevis. J. Embryol. Exp. Morphol.* **89 Suppl**, 185-209.

Kieny, M., Mauger, A., Chevallier, A. and Pautou, M. P. (1988). Origin and development of avian skeletal musculature. *Reprod. Nutr. Dev.* **28**, 673-686.

Koseki, H., Wallin, J., Wilting, J., Mizutani, Y., Kispert, A., Ebensperger, C., Herrmann, B. G., Christ, B. and Balling, R. (1993). A role for Pax-1 as a mediator of notochordal signals during the dorsoventral specification of vertebrae. *Development* **119**, 649-660.

Langman, J. and Nelson, G. R. (1968). A radioautographic study of the development of the somite in the chick embryo. *J. Embryol. exp. Morph.* **19**, 217-226.

Lin, Z., Lu, M. H., Schultheiss, T., Choi, J., Holtzer, S., DiLullo, C., Fischman, D. A. and Holtzer, H. (1994). Sequential appearance of muscle-specific proteins in myoblasts as a function of time after cell division: Evidence for a conserved myoblast differentiation program in skeletal muscle. *Cell Motil. Cytoskel.* **29**, 1-19.

Marcelle, C., Stark, M. R. and Bronner-Fraser, M. (1997). Coordinate actions of BMPs, Wnts, Shh and noggin mediate patterning of the dorsal somite. *Development* **124**, 3955-3963.

Meunsterberg, A. E., Kitajewski, J., Bumcrot, D. A., McMahon, A. P. and Lassar, A. B. (1995). Combinatorial signaling by Sonic hedgehog and Wnt family members induces myogenic bHLH gene expression in the somite. *Genes Dev.* **9**, 2911-2922.

Moore, S. W., Keller, R. E. and Koehl, M. A. (1995). The dorsal involuting marginal zone stiffens anisotropically during its convergent extension in the gastrula of *Xenopus laevis*. *Development* **121**, 3131-3140.

Nüsslein-Volhard, C. and Roth, S. (1989). Axis determination in insect embryos. *CIBA Found. Symp.* **144**, 37-55; discussion 55-64, 92-38.

Ordahl, C. P. (1993). Myogenic lineages within the developing somite. In *Molecular Basis of Morphogenesis* (ed. M. Berfield), pp. 165-176. New York: John Wiley and Sons.

Ordahl, C. P. and Le Douarin, N. M. (1992). Two myogenic lineages within the developing somite. *Development* **114**, 339-353.

Ordahl, C. P. and Williams, B. A. (1998). Knowing chops from chuck: roasting myoD redundancy. *BioEssays* **20**, 357-362.

Ordahl, C. P., Williams, B. A. and Denetclaw, W. F., Jr. (2000). Determination and morphogenesis in myogenic progenitor cells: an experimental embryological approach. In Somitogenesis Part 2, *Current Topics in Developmental Biology*, vol. 48 (ed. C. Ordahl) (Series Editors: R. A. Pederson and G. P. Schatten), pp. 319-367. Academic Press, Inc.

Ott, M., Bober, E., Lyons, G., Arnold, H. and Buckingham, M. (1991). Early expression of the myogenic regulatory gene, myf-5, in precursor cells of skeletal muscle in the mouse embryo. *Development* **111**, 1097-1107.

Palmeirim, I., Henrique, D., Ish-Horowicz, D. and Pourquie, O. (1997). Avian hairy gene expression identifies a molecular clock linked to vertebrate segmentation and somitogenesis. *Cell* **91**, 639-648.

Pourquie, O., Coltey, M., Teillet, M.-A., Ordahl, C. and Le Douarin, N. (1993). Control of dorsoventral patterning of somitic derivatives by notochord and floor plate. *Proc. Nat. Acad. Sci., USA* **90**, 5242-5246.

Pownall, M. and Emerson, C. (1992). Sequential activation of myogenic regulatory genes during somite morphogenesis in quail embryos. *Dev. Biol.* **151**, 67-79.

Roth, S., Stein, D. and Neusslein-Volhard, C. (1989). A gradient of nuclear localization of the dorsal protein determines dorsoventral pattern in the Drosophila embryo. *Cell* **59**, 1189-1202.

Seno, T. (1961). An experimental study on the formation of the body wall in the chick. *Acta Anat.* **45**, 60-82.

Smith, T. H., Kachinsky, A. M. and Miller, J. B. (1994). Somite subdomains, muscle cell origins, and the four muscle regulatory factor proteins. *J. Cell Biol.* **127**, 95-105.

Spence, M. S., Yip, J. and Erickson, C. A. (1996). The dorsal neural tube organizes the dermamyotome and induces axial myocytes in the avian embryo. *Development* **122**, 231-241.

Stern, H. M., Brown, A. M. and Hauschka, S. D. (1995). Myogenesis in paraxial mesoderm: preferential induction by dorsal neural tube and by cells expressing Wnt-1. *Development* **121**, 3675-3686.

Straus, W. L., Jr. and Rawles, M. E. (1953). An experimental study of the origin of the trunk musculature and ribs in the chick. *Am. J. Anat.* **92**, 471-509.

Tajbakhsh, S., Rocancourt, D. and Buckingham, M. (1996). Muscle progenitor cells failing to respond to positional cues adopt non-myogenic fates in *myf-5* null mice. *Nature* **384**, 266-270.

Tajbakhsh, S., Rocancourt, D., Cossu, G. and Buckingham, M. (1997). Redefining the genetic hierarchies controlling skeletal myogenesis: Pax-3 and Myf-5 act upstream of MyoD. *Cell* **89**, 127-138.

Teillet, M., Watanabe, Y., Jeffs, P., Duprez, D., Lapointe, F. and Le Douarin, N. M. (1998). Sonic hedgehog is required for survival of both myogenic and chondrogenic somitic lineages. *Development* **125**, 2019-2030.

Teillet, M. A. and Le Douarin, N. M. (1983). Consequences of neural tube and notochord excision on the development of the peripheral nervous system in the chick embryo. *Dev. Biol.* **98**, 192-211.

Tosney, K. W. (1994). Abstract. *J. Cell Biochem*. **188 Suppl.** 462.

Tosney, K. W., Dehnbostel, D. B. and Erickson, C. A. (1994). Neural crest cells prefer the myotome's basal lamina over the sclerotome as a substratum. *Dev. Biol.* **163**, 389-406.

Viallet, J. P., Prin, F., Olivera-Martinez, I., Hirsinger, E., Pourquiae, O. and Dhouailly, D. (1998). Chick Delta-1 gene expression and the formation of the feather primordia. *Mech. Dev.* **72**, 159-168.

Williams, B. A. and Ordahl, C. P. (1994). Pax-3 expression in segmental mesoderm marks early stages in myogenic cell specification. *Development* **120**, 785-796.

Williams, L. W. (1910). The somites of the chick. *Am. J. Anat.* **11**, 55-100.

Wolpert, L. (1969). Positional information and the spatial pattern of cellular differentiation. *J. Theor. Biol.* **25**, 1-47.

Wolpert, L. (1996). One hundred years of positional information. *Trends Genet.* **12**, 359-364.